Pramāṇa – J. Phys., Vol. 25, No. 6, December 1985, pp. 745–754. © Printed in India.

Properties of hard disc fluids by Baxter's method

B B DEO and B P DAS*

Department of Physics, Utkal University, Bhubaneswar 751 004, India
*Department of Physics, B.J.B. College, Bhubaneswar 751 014, India

MS received 8 June 1985; revised 27 September 1985

Abstract. The radial distribution function and the equation of state for hard disc fluids have been calculated at various densities by solving Ornstein-Zernike equation using Baxter's method.

Keywords. Radial distribution function; hard-discs; Baxter's formalism; Ornstein-Zernike equation.

PACS No. 51·90

1. Introduction

In recent years, the determination of the radial distribution function and the thermodynamic properties of two-dimensional fluids have been a subject of considerable interest. The two-dimensional fluid is often used as a model substance in the investigation of surface phenomena and more importantly to know the extent to which dimensionality of the system affects the nature of phase transition.

Valuable information concerning the equation of state and the radial distribution function for hard discs are now available with the advent of high-speed computers. Lado (1968), Chae *et al* (1969), Steele (1976) and others have reported the results of their computer calculations. But the disadvantages of these computer calculations are that they take long hours on even the fastest machines. Hence there is need to develop a simple but efficient method of calculating the thermodynamic properties of hard disc fluids.

The solution of the Ornstein-Zernike (O–Z) equation with Percus-Yevick (P-Y) closure has been found to be quite accurate and satisfactory for predicting the fluid properties in three dimensions. However in two dimensions it becomes difficult to obtain both analytic and numerical solutions of the O-Z equation.

The approximate theory of Reiss *et al* (1959) known as scaled particle theory (SPT) for hard spheres has been extended by Helfand *et al* (1961) for hard discs and rods. This theory gives reasonably good predictions for the equations of state. For hard discs from SPT we get the expression for the equation of state.

$$p_v/k_BT = \rho/(1-y)^2 \tag{1}$$

where $y = \pi/4 \cdot \rho \cdot \sigma^2$; ρ being the particle number density and σ is the disc diameter.

Later Henderson (1975) empirically modified this equation and obtained a more accurate expression for the hard disc equation of state viz

$$p_v/k_BT = \rho\left(1+\frac{y^2}{8}\right)\Big/(1-y)^2. \tag{2}$$

However, the solution of the O–Z equation by Wiener-Hopf factorization suggested by Baxter (1968) yielded astonishingly satisfactory results for hard-sphere fluids and fluids with realistic potentials. The amazing success of Baxter's formalism encouraged us to extend his formalism to the case of hard discs.

In the present work, we have suggested a method which is more accurate than those of Thompson and Freasier (1980). We have numerically evaluated the radial distribution function $g(r)$, the direct correlation function $c(r)$ and p/k_BT from the virial and compressibility equations of state and have compared them with those obtained by computer calculations.

2. O–Z equation

The O–Z equation in two dimensions is given by

$$h(\mathbf{r}) = c(\mathbf{r}) + \rho \int \mathrm{d}\mathbf{s}\, c(\mathbf{s}) h(|\mathbf{r}-\mathbf{s}|), \tag{3}$$

where $h(r)$ $[= g(r)-1]$ is the indirect correlation function and $c(r)$ is the direct correlation function. The closure is made either by the Percus-Yevick (P-Y) equation

$$c(r) = g(r)\cdot[1-\exp(\phi(r)/k_BT)], \tag{4}$$

or by the hypernetted-chain (HNC) equation

$$c(r) = h(r) - \ln g(r) - \phi(r)/k_BT. \tag{5}$$

where $\phi(r)$ is the inter-atomic potential, k_B the Boltzmann's constant and T the temperature. Of the two closures the P-Y closure is simpler and perhaps more accurate and reliable.

The solution of the O–Z equation can be used to determine several thermodynamic properties. The expression for the two-dimensional pressure can be obtained either from the two-dimensional virial equation of state

$$p_v/k_BT = \rho - \frac{\pi\rho^2}{2k_BT}\int_0^\infty \frac{\mathrm{d}\phi}{\mathrm{d}r} g(r) r^2\, \mathrm{d}r. \tag{6}$$

or from the two-dimensional compressibility equation of state

$$\frac{1}{k_BT}(\partial p/\partial\rho)_T = \left[1 + 2\pi\rho\int_0^\infty (g(r)-1) r\, \mathrm{d}r\right]^{-1}. \tag{7}$$

The disadvantage of the P-Y approximation is that the virial and the compressibility pressures calculated from these equations do not agree. Nevertheless, it is quantitatively fairly reliable for short range potentials.

3. Baxter's method

The Fourier transform of the O–Z equation is

$$\tilde{h}(k) = \tilde{c}(k) + \rho\tilde{c}(k)\tilde{h}(k), \tag{8}$$

where $$\tilde{h}(k) = 2\pi \int_0^\infty h(r) J_0(kr) r \, dr, \tag{9}$$

$$\tilde{c}(k) = 2\pi \int_0^\infty c(r) J_0(kr) r \, dr, \tag{10}$$

are the zeroth order Henkel transforms of $h(r)$ and $c(r)$ respectively. $J_0(kr)$ is the zeroth order Bessel function of the first kind.

To solve the O–Z equation a function $\tilde{A}(k)$ is introduced such that

$$\tilde{A}(k) = 1 - \rho \tilde{c}(k) = [1 + \rho \tilde{h}(k)]^{-1}. \tag{11}$$

As suggested by Baxter (1968), a Wiener-Hopf factorization of $\tilde{A}(k)$ is carried out as:

$$\tilde{A}(k) = \tilde{Q}(k)\tilde{Q}(-k). \tag{12}$$

The function $\tilde{Q}(k)$ is analytic in the upper half of the complex K-plane and has zeros only in the lower half of the plane whereas $\tilde{Q}(-k)$ is analytic in the lower half of the complex K-plane and has zeros only in the upper half of the plane.

The inverse one-dimensional Fourier transform of $\tilde{Q}(k)$ s defined as,

$$\begin{aligned} Q(r) &= 0 \qquad \text{for} \quad r < 0 \\ &= \frac{1}{4\pi^2 \rho} \int_{-\infty}^{+\infty} [1 - \tilde{Q}(k)] \exp(-ikr) dk \quad \text{for} \quad r > 0. \end{aligned} \tag{13}$$

The function $Q(r)$ is a real function, is continuous except at $r = 0$, and tends to zero as r tends to infinity.

The inverse Fourier transform of $\tilde{h}(k)$ and $\tilde{c}(k)$ are given by

$$\begin{aligned} J(|r|) &= \frac{1}{4\pi^2} \int_{-\infty}^{+\infty} \exp(-ikr) \tilde{h}(k) dk \\ &= \frac{1}{\pi} \int_{|r|}^{\infty} \frac{t h(t) dt}{\{t^2 - r^2\}^{1/2}}, \end{aligned} \tag{14}$$

and

$$\begin{aligned} S(|r|) &= \frac{1}{4\pi^2} \int_{-\infty}^{+\infty} \exp(-ikr) \tilde{c}(k) dk \\ &= \frac{1}{\pi} \int_{|r|}^{\infty} \frac{t c(t) dt}{\{t^2 - r^2\}^{1/2}}. \end{aligned} \tag{15}$$

Upon rewriting (11) and (12) as

$$1 - \rho \tilde{c}(k) = \tilde{Q}(k)\tilde{Q}(-k),$$

and

$$[1 + \rho \tilde{h}(k)] \tilde{Q}(k) = \frac{1}{\tilde{Q}(-k)},$$

and performing inverse Fourier transform, we get

$$J(r) = Q(r) + 2\pi\rho \int_0^\infty dt \, Q(t) J(|r - t|), \tag{16}$$

$$S(r) = Q(r) + 2\pi\rho \int_0^\infty dt \, Q(t) Q(t - r). \tag{17}$$

The indirect correlation function $h(r)$ and the direct correlation function $c(r)$ can be obtained from the inverse Abel transform of equations (14) and (15) as

$$h(r) = -2\int_r^\infty \frac{J'(x)\mathrm{d}x}{\{x^2-r^2\}^{1/2}}, \tag{18}$$

$$c(r) = -2\int_r^\infty \frac{S'(x)\mathrm{d}x}{\{x^2-r^2\}^{1/2}}, \tag{19}$$

where $J'(x)$ and $S'(x)$ are the first derivatives of $J(x)$ and $S(x)$ respectively.

4. Thermodynamic properties

The compressibility equation of state (7) can be written in conjunction with equations (9), (11) and (12) as

$$\begin{aligned}\frac{1}{k_BT}\left(\frac{\partial p}{\partial \rho}\right)_T &= [1+\rho\textstyle\int_0^\infty h(r)\,2\pi r\,\mathrm{d}r]^{-1}\\ &= [1+\rho\tilde{h}(0)]^{-1}\\ &= 1-\rho\tilde{c}(0)\\ &= [\tilde{Q}(0)]^2,\end{aligned} \tag{20}$$

where $$\tilde{Q}(0) = 1-2\pi\rho\textstyle\int_0^\infty Q(r)\mathrm{d}r. \tag{21}$$

Expressions for the virial and the compressibility pressures for the hard discs can be obtained from (6) and (20) as

$$p_v/k_BT = \rho + \tfrac{1}{2}\pi\rho^2\sigma^2 g(\sigma_+), \tag{22}$$

$$p_c/k_BT = \textstyle\int_0^\rho [k_BT(\partial\rho/\partial p)_T]^{-1}\mathrm{d}\rho, \tag{23}$$

where $g(\sigma_+)$ is the contact value of the radial distribution function.

We shall evaluate both these equations and explicitly show that they are different as in the case of three dimensions.

5. Numerical procedure

The r axis is divided into two regions, the core-region ($0 < r < \sigma$) and a tail region ($\sigma < r < \infty$). For the start of the iteration the initial values of different functions, following Thompson (1980) are taken as:

$$\begin{aligned} h_i(r) &= -1 && \text{for } r < \sigma,\\ &= 0 && \text{for } r > \sigma,\\ c_i(r) &= 0 && \text{for } r > \sigma,\\ Q_i(r) &= 0 && \text{for } r > \sigma,\\ J_i(r) &= -\frac{(\sigma^2-r^2)^{1/2}}{\pi} && \text{for } r < \sigma,\\ &= 0 && \text{for } r > \sigma, \end{aligned}$$

and $S_i(r) = 0 \quad$ for $\quad r < \sigma.$

Then the following steps are followed to calculate the functions $h(r)$, $c(r)$, $\tilde{h}(k)$ and $\tilde{c}(k)$.

Step 1.

The new values of $Q(r) = Q_n(r)$ for $r < \sigma$ are found from

$$Q_n(r) = J_i(r) - 2\pi\rho \int_0^\sigma \mathrm{d}t\, Q_i(t) J_i(|r-t|),$$

and then we set $Q_i(r) = Q_n(r)$.

Step 2.

The new values of $J(r) = J_n(r)$ for $r > \sigma$ are found from

$$J_n(r) = 2\pi\rho \int_0^\sigma \mathrm{d}t\, Q_i(t) J_i(r-t),$$

and then we set $J_i(r) = J_n(r)$.

Step 3.

The new values of $h(r) = h_n(r)$ for $r > \sigma$ are found from

$$h_n(r) = -2 \int_r^R \frac{J_i'(t)\,\mathrm{d}t}{\{t^2 - r^2\}^{1/2}},$$

and then we set $h_i(r) = h_n(r)$.

Step 4.

The values of $S(r) = S_n(r)$ for $r < \sigma$ are found from

$$S_n(r) = Q_i(r) - 2\pi\rho \int_r^\sigma Q_i(t) Q_i(t-r)\mathrm{d}t,$$

and then we set $S_i(r) = S_n(r)$

Step 5.

New values of $C(r) = C_n(r)$ for $r < \sigma$ are calculated from

$$C_n(r) = -2 \int_r^\sigma \frac{S_i'(t)\,\mathrm{d}t}{\{t^2 - r^2\}^{1/2}},$$

and then we set $C_i(r) = C_n(r)$.

Step 6.

The values of $J(r) = J_n(r)$ for $r < \sigma$ are calculated from (14)

$$J_n(r) = \frac{1}{\pi} \int_r^\infty \frac{t h(t)\,\mathrm{d}t}{\{t^2 - r^2\}^{1/2}}.$$

The evaluation of this $J_n(r)$ for $r < \sigma$ is the most crucial in the present scheme of iteration and we would like to elaborate on this point.

The discontinuity in $h(r)$ at $r = \sigma$ poses difficulties in the numerical computation of $J(r)$. For $t > \sigma$, Thompson and Freasier (1980) have evaluated $J(r)$ by integrating by parts the Abel transform which gives

$$J(r) = \frac{1}{\pi}\int_{\sigma}^{\infty} [t^2 - r^2]^{1/2} h'(t)\mathrm{d}t, \tag{24}$$

which involves an extra integration

$$h(r) = -\int_{r}^{\infty} h'(t)\mathrm{d}t. \tag{25}$$

For $t < \sigma$, they have used

$$J(r) = -\left(\frac{1 + h(\sigma_+)}{\pi}\right)(\sigma^2 - r^2)^{1/2}, \tag{26}$$

where $h(\sigma_+)$ is the contact value of $h(r)$ just outside the hard core.

We have found that all this unnecessarily complicates the evaluation. Instead, we have proceeded as follows:

for $t < \sigma$ $J(r) = -(\sigma^2 - r^2)^{1/2}/\pi$, (27)

and for $t > 2\sigma$ $$J(r) = \frac{1}{\pi}\int_{2\sigma}^{\infty}\left[h(t)\left(\frac{t-r}{t+r}\right)^{1/2} + r\frac{h(t)}{(t^2 - r^2)^{1/2}}\right]\mathrm{d}t. \tag{28}$$

In the sensitive region between σ and 2σ we have overcome the difficulty in the t-integration by writing,

$$J(r) = \frac{1}{\pi}\int_{\sigma}^{2\sigma} \frac{[t\,h(t) - r\,h(r)]}{(t^2 - r^2)^{1/2}}\mathrm{d}t + \frac{1}{\pi} r h(r)\int_{\sigma}^{2\sigma} \frac{\mathrm{d}t}{(t^2 - r^2)^{1/2}} \tag{29}$$

Proceeding in this manner convergence in the value of $J(r)$ is much better and is achieved after the third iteration.

The virial and the compressibility pressures were evaluated using (20), (22), (23) and the following relation results

$$\tilde{Q}(0) = 1 - 2\pi\rho\int_0^{\sigma} Q(r)\mathrm{d}r.$$

6. Results

The results are graphically shown in figures 1, 2 and 3. Figure 1 shows the comparative graphs for $g(r)$ and r at $\rho\sigma^2 = 0{\cdot}693$ plotted from present calculations and from the results of Chae *et al* (1969) using P-Y integral equation. In figure 2, $p/\rho k_B T$ evaluated from the virial and the compressibility equations (22) and (23), have been plotted against various densities according to the present findings and the findings of Lado (1968). In figure 3, $k_B T\,(\partial\rho/\partial p)_T$ has been plotted against various densities according to the present findings and those of Lado (1968).

The values of $Q(r)$ and $C(r)$ at different r for various densities are plotted in figures 4 and 5. These results are new and have never been reported before. The nature of

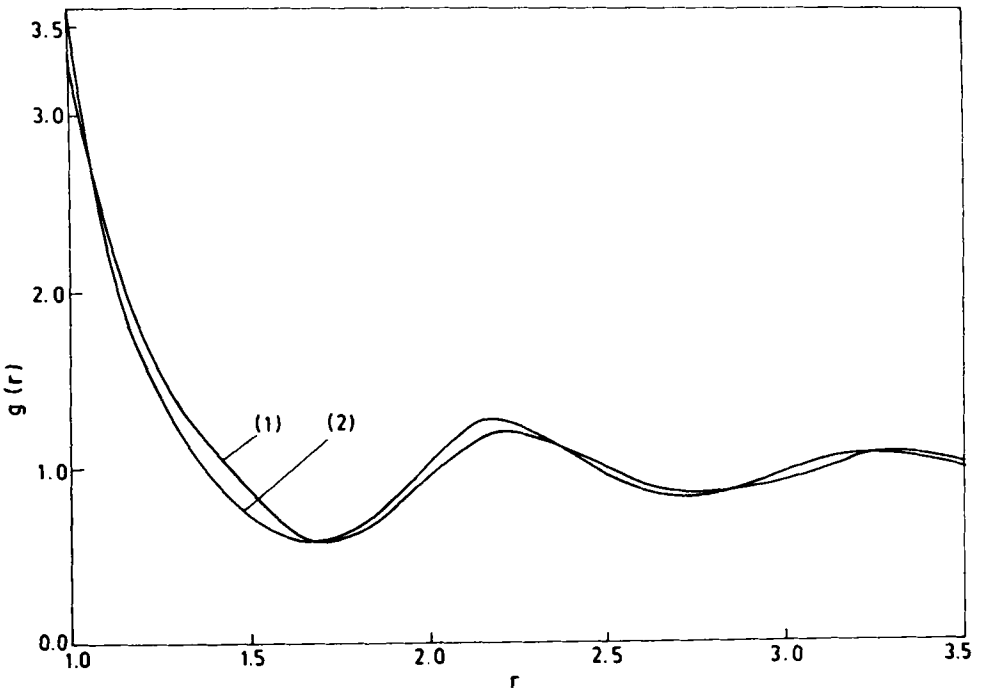

Figure 1. Plot of $g(r)$ with r at $\rho\sigma^2 = 0{\cdot}693$ as obtained in the present work (1) and from the solution of the P-Y integral equation (2) (Chae *et al* 1969)

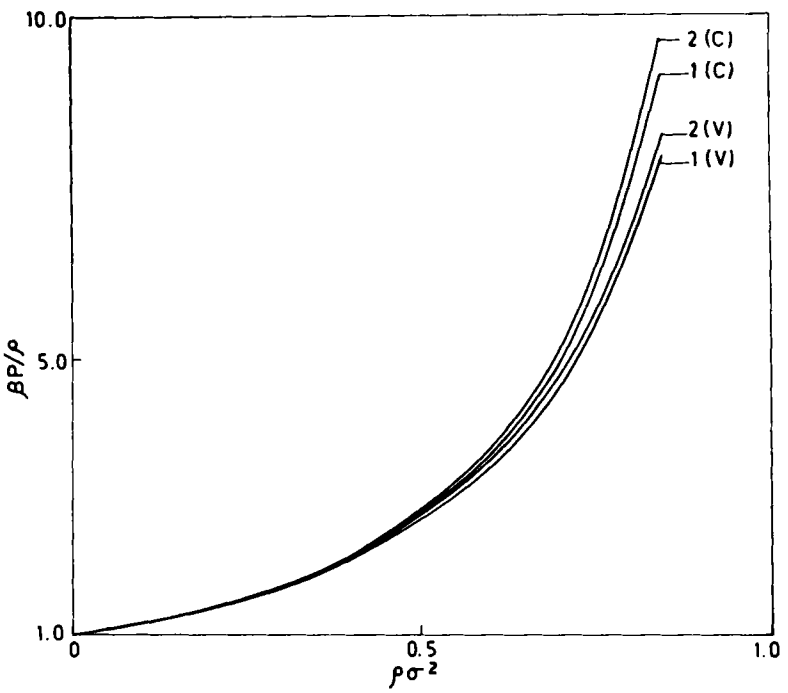

Figure 2. Plot of the virial and the compressibility equations of state with density as obtained in the present calculation [1(V) and 1(C)], and from the solution of P-Y integral equation [2(V) and 2(C)] (Lado 1968).

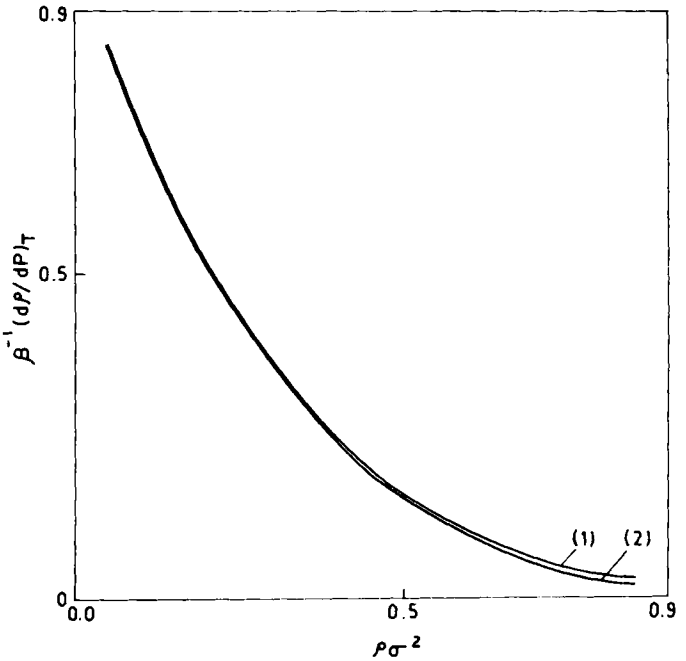

Figure 3. Plot of isothermal compressibilities with density as obtained in the present work (1) and from the solution of P-Y integral equation (2) (Lado 1968).

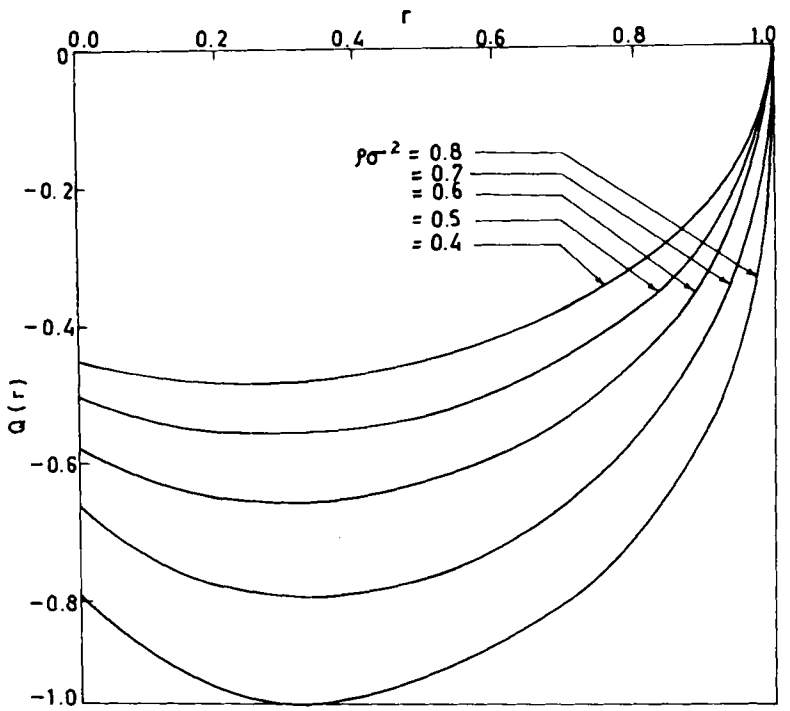

Figure 4. Plot of $Q(r)$ with r at various densities.

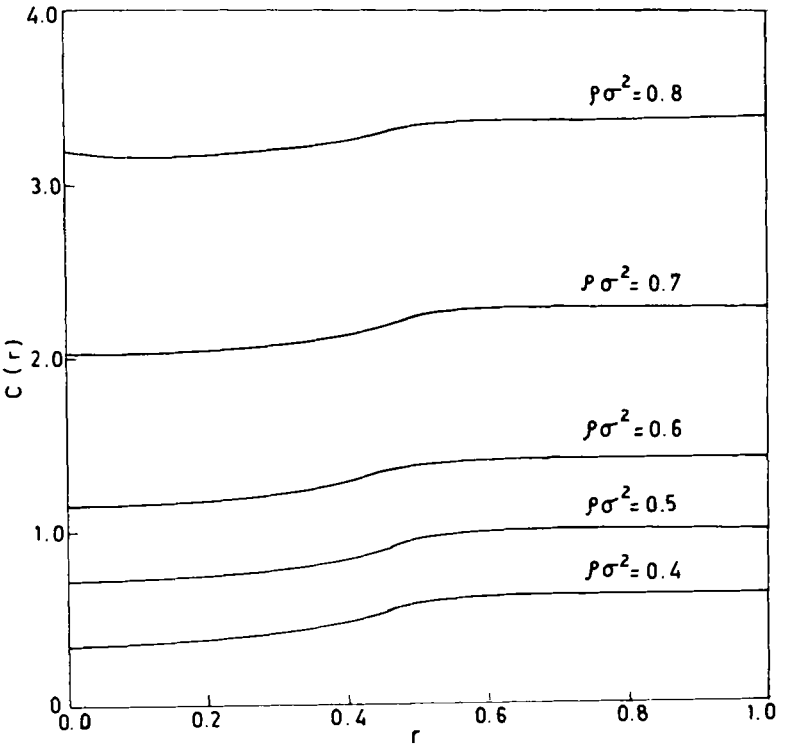

Figure 5. Plot of $C(r)$ with r at various densities.

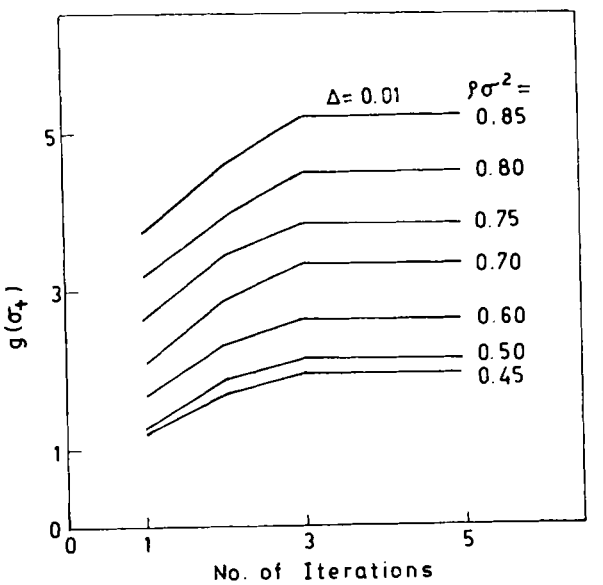

Figure 6. Plot of $g(\sigma_+)$ with the number of iterations.

Table 1.

$\rho\sigma^2$	$p/\rho k_B T$				
	Virial			Compressibility	
	Present method	Lado (1968)	Chae *et al* (1969)	Present method	Lado (1968)
0·45	2·39	2·4	2·36 (at $\rho\sigma^2 = 0{\cdot}444$)	2·44	2·44
0·5	2·7	2·71	2·72	2·76	2·77
0·6	3·52	3·54	3·604	3·68	3·70
0·7	4·75	4·79	4·73	5·12	5·16
0·75	5·62	5·67	5·45 (at $\rho\sigma^2 = 0{\cdot}745$)	6·17	6·24
0·8	6·73	6·80	..	7·60	7·68
0·85	8·14	8·26	..	9·51	9·65

convergence is shown in figure 6, where the value of the radial distribution function close to σ, $g(\sigma_+)$ is plotted against the number of iterations for reduced densities from $\rho\sigma^2 = 0{\cdot}45$ to 0·85.

7. Discussion

By using equation (29), it was found that the result converged right from the third iteration, as is evident from figure 6. The calculations were repeated for different step sizes and for small grid spacings and the results were found to be independent of the step size.

The computed values of the reduced virial and compressibility pressures by the present method are listed and compared with those of Lado and Chae *et al* in table 1. As is evident from the table, the difference between the present values and those of Lado and Chae *et al* is within 2%. Lado's estimation of error in his results is less than 0·5% for low densities and 2% for higher densities.

Since the final values are quite stable both for changes in grid spacing and the number of iterations, the major part of the difference is likely to be the errors in computer calculations.

The merit of this method will be further examined when an attractive potential is included along with the hard core.

References

Baxter R J 1968 *Aust. J. Phys.* **21** 563
Chae D G, Ree F H and Ree T 1969 *J. Chem. Phys.* **50** 1581
Helfand E, Frisch H L and Lebowitz J L 1961 *J. Chem. Phys.* **34** 1037
Henderson D 1975 *Mol. Phys.* **30** 971
Lado F 1968 *J. Chem. Phys.* **49** 3092
Reiss H, Frisch H L and Lebowitz J L 1959 *J. Chem. Phys.* **31** 369
Steele W A 1976 *J. Chem. Phys.* **65** 5256
Thompson N E and Freasier B C 1980 *Mol. Phys.* **41** 127